Phase separation in SiGe nanocrystals embedded in SiO_2 matrix during high temperature annealing

N. A. P. Mogaddam,[1,a)] A. S. Alagoz,[1,3] S. Yerci,[1,4] R. Turan,[1] S. Foss,[2] and T. G. Finstad[2]
[1]*Department of Physics, Middle East Technical University, 06531 Ankara, Turkey*
[2]*Department of Physics, University of Oslo, Oslo 0316, Norway*
[3]*Department of Applied Science, University of Arkansas at Little Rock, Little Rock, Arkansas 72204, USA*
[4]*Department of Electrical and Computer Engineering, Boston University, Boston, Massachusetts 02215, USA*

(Received 14 July 2008; accepted 5 November 2008; published online 19 December 2008)

SiGe nanocrystals have been formed in SiO_2 matrix by cosputtering Si, Ge, and SiO_2 independently on Si substrate. Effects of the annealing time and temperature on structural and compositional properties are studied by transmission electron microscopy, x-ray diffraction (XRD), and Raman spectroscopy measurements. It is observed that Ge-rich $Si_{(1-x)}Ge_x$ nanocrystals do not hold their compositional uniformity when annealed at high temperatures for enough long time. A segregation process leading to separation of Ge and Si atoms from each other takes place. This process has been evidenced by a double peak formation in the XRD and Raman spectra. We attributed this phase separation to the differences in atomic size, surface energy, and surface diffusion disparity between Si and Ge atoms leading to the formation of nonhomogenous structure consist of a Si-rich SiGe core covered by a Ge-rich SiGe shell. This experimental observation is consistent with the result of reported theoretical and simulation methods. © *2008 American Institute of Physics*.
[DOI: 10.1063/1.3048543]

I. INTRODUCTION

In recent years, Si, Ge, and their alloy nanostructures embedded in a dielectric matrix have widely been investigated because of their potential application in nanoelectronics and optoelectronics.[1,2] In particular, the use of nanocrystals in flash memory cells instead of conventional floating gate is expected to improve the device reliability.[3] Alloy SiGe nanocrystals provide an advantage of fine tuning the electronic band structure, which plays a detrimental role in the charging/discharging and retention properties of the memory element.[4] In order to fabricate high performance devices with SiGe nanocrystals, it is necessary to know and control their structural and electrical properties,[5,6] which depend on several factors including particle size, shape, surface condition, atomic composition, and compositional uniformity. Considering only thermodynamics of bulk materials, homogenous SiGe nanocrystals embedded in a SiO_2 matrix would be an equilibrium situation.[1] This situation was also reported for annealing SiO_2 supersaturated by Si and Ge using ion implantation[7] or sputtering.[8] Other structures can be thought to exist in such material system when taking surface effects and kinetics into consideration. There have been several theoretical studies on clusters of SiGe alloys indicating that a core-shell structure can be more stable than a homogenous structure.[9,10]

In the past few years, much effort has been focused on the synthesis, fabrication, and characterization of the core-shell structures with tailored applications.[6,11] At high Ge content, for samples prepared by rf magnetron cosputtering and annealed at high temperatures, no homogeneous nc-$Si_{(1-x)}Ge_x$ but a kind of composite nanocrystals consisting of a nanocrystals (nc)-Ge core and amorphous SiGe shell evidenced from the Raman analysis was reported.[12,13] From other experiments, Alonso *et al.*[14] by using molecular beam epitaxy (MBE) method and Malachias *et al.*[15] by using chemical etching method observed dome islands that present a spherical profiles consisting of a Si-rich core covered by a Ge-rich shell. In more recent experiments, SiGe self-assembled islands composed of strained Ge core and a more relaxed SiGe shell prepared by MBE method were reported.[16,17] A composition gradient in the SiGe nanocrystals can possibly arise by high temperature treatment of SiGe nanocrystals in SiO_2 on Si where several effects may contribute to the end results, which could be different than those for a free SiGe particle. There is possibly a flux to and from the particles resulting in Oswald ripening, which will be influenced by the different surface energies of small and large particles as well as Si or Ge bonds on the particle surface. These fluxes are coupled to flux to and from the substrate involving epitaxial growth on the substrate and a possible particle flux that can react with species from the ambient during annealing forming some new oxide.[18]

We studied the effect of annealing time and temperature on the structural and compositional properties of SiGe nanocrystals prepared by rf magnetron cosputtering method by transmission electron microscopy (TEM), x-ray diffraction (XRD), and Raman spectroscopy measurements. The evolution of SiGe nanocrystals has been monitored during high temperature annealing. Results indicate that a phase separation of Si and Ge takes place during enough long high temperature annealing or cooling down process leading to an inhomogeneous structure consist of a Si-rich SiGe core covered by a relatively Ge-rich SiGe shell.

[a)]Electronic mail: nasghar@newton.physics.metu.edu.tr.

II. EXPERIMENTAL DETAILS

The samples used in this work were SiGe rich SiO_2 layer sandwiched between two SiO_2 films deposited on Si substrate by rf magnetron cosputtering from three independent target materials with powers of $P_{SiO_2}=350$ W, $P_{Si}=100$ W, and $P_{Ge}=20$ W. The bottom SiO_2 layer with the thickness of about 40 nm was deposited on Si to restrain Ge atoms from growing epitaxially on the Si substrate in the postannealing process. The top SiO_2 layer with the thickness of about 40 nm was deposited to impede the diffusion of Ge atoms out of the surface. Deposition parameters were fixed to study the effect of annealing time on the local structure of the samples. The typical deposition rate was 4 nm/min and the thickness of the films was about 350 nm. The x-ray photoemission spectroscopy (XPS) depth profile of the as-grown sample is carried out to obtain the relative elemental concentration. Equipping Specs XPS system at a vacuum of 1×10^{-7} Pa depth profiles of Si, Ge, O, and C atoms were recorded. After three time sputtering with 2000 eV Ar^+ ions with the cycle of 2 min followed by a 4 min 3500 eV sputtering, the steady state elemental composition values of 32.9, 19, 48.1, and 0% have been obtained for Si, Ge, O, and C atoms, respectively.

After deposition, wafers were cleaved and annealed in a quartz tube furnace under flowing N_2 gas at ambient pressure for 1, 3, and 5 h at 1100 °C. High annealing temperatures (1100 °C) were chosen to understand compositional variations in the nanocrystals in the prolonged high temperature regime. In general, the formation mechanism for SiGe nanocrystals embedded in SiO_2 matrix goes through the familiar sequence of nucleation and growth, often followed by coarsening of nanocrystals due to Ostwald ripening. The formation and evolution of SiGe nanostructures were studied by cross-sectional high-resolution electron microscope (JEOL2010F). X-ray diffraction measurements were carried out with the Cu $K\alpha$ line of a powder diffractometer to obtain conventional θ-2θ scans between 24°–31° and 44°–56° at 0.01 steps. This range of 2θ was scanned by long acquisition time per angular step of 15 s to obtain the exact position and full width at half maximum of the peaks correspond to (111), (220), and (311) diffractions. Raman scattering spectra were taken on a confocal micro-Raman (HR800, Jobin Yvon), attached with Olympus microanalysis system and a charge-coupled device camera providing a resolution of ~1 cm^{-1}. The spectra were carried out in backscattering geometry with the 632.8 nm line of He–Ne laser at room temperature.

III. RESULTS AND DISCUSSION

Among the various sets of samples, in a set with sputtering parameters of $P_{SiO_2}=350$ W, $P_{Si}=100$ W, and $P_{Ge}=20$ W (leading to the formation of Ge-rich $Si_{(1-x)}Ge_x$ nanocrystals) and annealed at 1100 °C for different duration of 1–5 h, an interesting feature has been observed. It was the deconvolution tendency of the SiGe related peaks in XRD and Raman measurements in the samples annealed for enough long times. This feature was examined by TEM measurements as well.

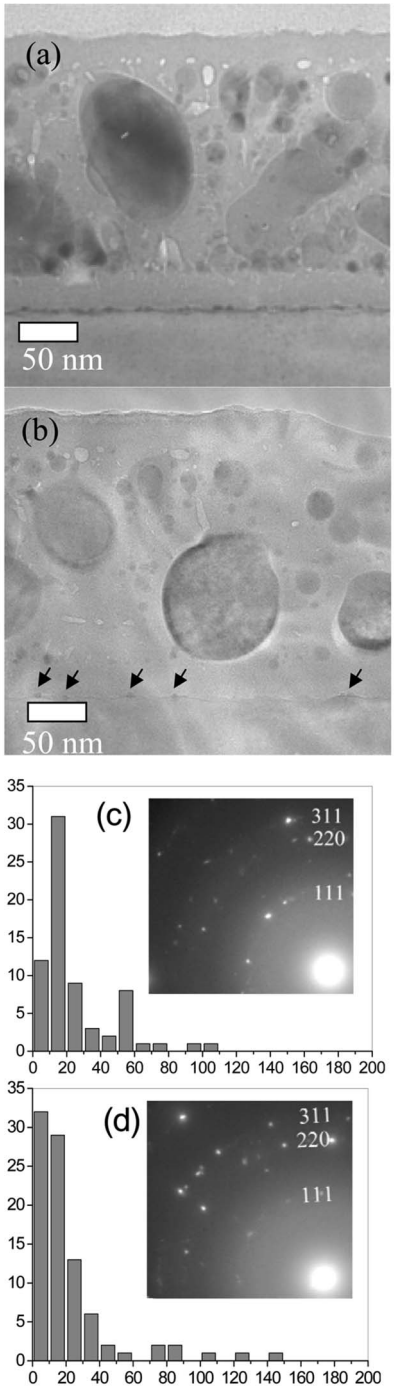

FIG. 1. Cross-sectional TEM image of the sample annealed at 1100 °C for 1 h (a) and 3 h (b) and size distribution of the nanocrystals in the sample annealed for 1 h (c) and 3 h (d). Insets show the selected area diffraction patterns.

A. Transmission electron microscopy

Figures 1(a) and 1(b) show the evolution of cross-sectional TEM image of the samples annealed at 1100 °C for 1 and 3h. The circular features seen have been identified to be SiGe nanocrystals from high resolution interference fringes and from selected area diffraction [insets of Figs. 1(c) and 1(d)]. Mixtures of nanocrystals of all sizes with the same average of 22 nm exist within the cosputtered layers. This large variation can be understood by the Ostwald ripening

process where large nanocrystals grow on behalf of the smaller ones, which shrink.[19] Size distribution comparison of these two samples indicates that [Figs. 1(c) and 1(d)] for the sample annealed for a long time of 3 h, the number of nanocrystals with sizes $\leq$10 nm is about three times of the sample annealed for 1h and also large nanocrystals with sizes $\sim$150 nm are formed accompanied by significant decrease in the number of nanocrystals having moderate size of 50 nm. The SiO_2 layer between the cosputtered layer and the substrate does not appear to contain Ge and/or SiGe nanocrystals. This is an expected feature for this annealing treatment, the concentrations in this SiO_2 layer will be less than the solid solubility so there is no driving force for segregation except perhaps during the cooling down process, but since there already exist segregation sites within a short diffusion distance the concentration can be kept close to equilibrium during a large portion of the cooling down process. So, comparing with the TEM image of the samples annealed at 900 and 1000 °C (not shown here) for 1h, thickness of the upper and bottom SiO_2 layers is slightly decreased and the interface between the SiO_2 and SiGe layers is no longer flat.

On the other hand, in the sample annealed for 1 h there is a distinctive layer identified as Ge and/or SiGe precipitated onto the Si substrate, which is supposed to be caused by Ge diffusion form the cosputtering layer. Regarding the dependency of diffusion length on parameters such as diffusivity of Ge atoms in SiO_2, annealing time, and temperature,[20,21] the sputtered pure SiO_2 layer did not act as a perfect diffusion barrier for Ge for this annealing regime. Diffusion of Ge atoms in SiO_2 and precipitated onto the Si substrate for samples annealed at elevated temperatures of 1000 °C and higher has reported many times and generally is related to the complete miscibility between Ge and Si at high annealing temperatures.[22,23] In the sample annealed for 3 h, the number of precipitants onto the Si substrate has been decreased and only some small spots have been observed (shown by arrows). We suggest and justify that this observation during prolonged annealing is a consequence of the intermixing between the precipitants and the Si substrate and formation of SiGe alloy. This is like epitaxial systems, in which there is a large thermodynamic driving force for intermixing because mixing reduces strain energy.[24,25] Prolonged high temperature annealing leads to increased elemental interdiffusion at the precipitant/substrate interface and allow an elemental redistribution so that the system can release strain energy as much as possible. Therefore, intermixing results in the precipitants/substrate interface moving down to the substrate side and dilution/dissolving of the precipitants.

The more striking feature in the TEM image of the sample annealed for 3 h shown in Fig. 1(b) is the dark contrast appeared around the nanocrystals with sizes greater than 50 nm. These types of contrasts are often observed in TEM showing precipitates and can arise by different effects pertaining to the analysis method. Interface electron scattering often causes similar contrasts. There is no direct evidence from TEM that the nanoparticle composition is different near the surface of the nanoparticle. On the other hand, it cannot be excluded. As will be discussed below, there may exist driving forces due to difference in atomic sizes and surface energy between Si and Ge, which may induce segregation of Ge to the surface of the nanocrystal. Also a bright contrast in the vicinity of the large islands, (like an outer shell) near to the bottom SiO_2 layers, can be attributed to the Si atoms diffused from the substrate. Existence of large number of voids (or pores) in sputtered silicon oxide (as can be seen in our sample in Fig. 1) is necessary for diffusion of the Si atoms in the silicon oxide matrix.[20,21]

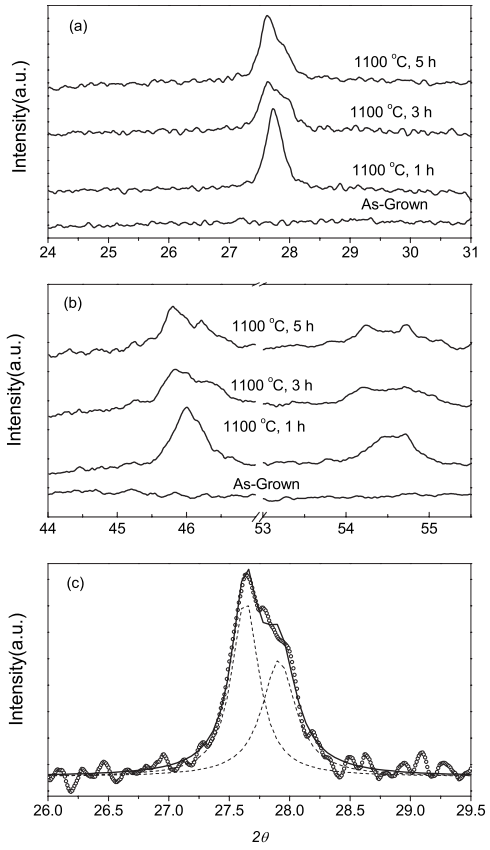

FIG. 2. XRD pattern of the as grown and the samples annealed at different times in the 2θ interval of 24°–31° corresponding to (111) planes (a), 44°–56° corresponding to (220) and (311) planes (b), and the decomposition of the (111) diffraction peak of the sample annealed for 3 h (c).

B. X-ray diffraction

Figure 2 shows XRD spectra for the samples annealed at 1100 °C for 1, 3, and 5 h. Three peaks can be resolved at $\sim$27.7°, 46°, and 54.5° [Fig. 2(a) and 2(b)], which are located between the expected (111), (220), and (311) Bragg peaks of Si and Ge. At first sight, while the XRD peak of the sample annealed for 1 h is a single diffraction peak corresponding to a single composition, in those of annealed for 3 and 5 h the XRD peak tends to decomposed into two peaks at 27.6° and 27.9°, respectively. By increasing annealing time from 3 h to 5 h, the intensity of the decomposed peak located at 27.9° does not change and that of located at 27.6° increases. This feature is seen more clearly for the peaks located at 46° and 54.5°, corresponding to (220) and (311) diffractions. This result indicates that in the sample annealed for 1 h, uniform SiGe nanocrystals with an approximate Ge content of $x=69$ have been formed. This value was obtained by means of the relationship between lattice constant and Ge

content, assuming that SiGe is fully relaxed.[26] However, because of the possible stress development on the nanocrystals, the actual value of x could be somewhat different. The evolution of the XRD peaks indicates a phase separation between Si and Ge. Figure 2(c) shows the decomposition of the (111) peak of the sample annealed for 3 h by two Lorentzian peaks. We attribute the peak at 27.6° to a portion containing more Ge atoms and the peak at 27.9° to that being relatively Si-rich. It is worth whiling to note that nanocrystals located at different depths in SiO_2 matrix measured from the electron beam entrance surface appear like nanocrystals having different Ge contents x. Although there exists a distribution in the Ge content of the islands, the explicit phase separation owing to different Ge content in the XRD pattern should lead to the appearance of duplex in selected area diffraction (SAD) fringes [inset of Figs. 1(c) and 1(d)]. SAD patterns of two samples do not show any explicit difference between them and pair fringes result from splitting of the diffraction rings has not observed.

By using the XRD signal corresponding to (111) diffraction of the sample annealed for 1 h we can estimate the mean crystallite size D and the root-mean-square strain $\langle e^2 \rangle^{1/2}$.[27] We obtained these quantities by using pseudo-Voigt function in the variance-range method from the following expressions:

$$w_{0f} = -\lambda^2 L/4\pi^2 \cos^2 \theta_0 D^2 + 4 \tan^2 \theta_0 \langle e^2 \rangle, \quad (1)$$

$$k_f = \lambda K/\pi^2 \cos \theta_0 D, \quad (2)$$

where w_{0f} and k_f are the intercept and slope parameters of the "pure" or "intrinsic" diffraction profile variance. The parameters K and L are related to the shape of the crystallites, and by assuming a spherical shape for the crystallites the values of $K=1.2090$ and $L=0$ have been used.[27] Besides the instrumental broadening correlation considered here, background and Cu $K\alpha 2$ line correlation have been applied as well.

We have obtained the values of 22 nm and 0.003 for mean crystallite size and root-mean-square strain, respectively, in a good agreement with the average value obtained by TEM. The observed strain can be attributed to the stretching of Si–Ge bonds (~2.4 Å) with respect to relaxed $Si_{(1-x)}Ge_x$ occurring near the nc-$Si_{(1-x)}Ge_x$/oxide interface due to the shorter Si–O bonds (~1.6 Å). On the other hand, annealing temperature is a critical parameter in evolution of SiGe nanocrystals. Regarding this, the melting point of $Si_{(1-x)}Ge_x$ alloy should be considered. It decreases with increasing Ge content. In our system, the liquidus-solidus diagram[28] shows that $Si_{0.31}Ge_{0.69}$ (or $Si_{0.35}Ge_{0.65}$ by Raman analysis) is in a partially melted state at 1100 °C. It is then reasonable to expect that volume expansion of SiGe during liquid to solid transition contribute to stress development on the nanocrystals.

C. Raman spectroscopy

We have also employed Raman spectroscopy to monitor the evolution of SiGe nanocrystals as displayed in Fig. 3. In general, the first-order Raman spectrum of a $Si_{1-x}Ge_x$ alloy

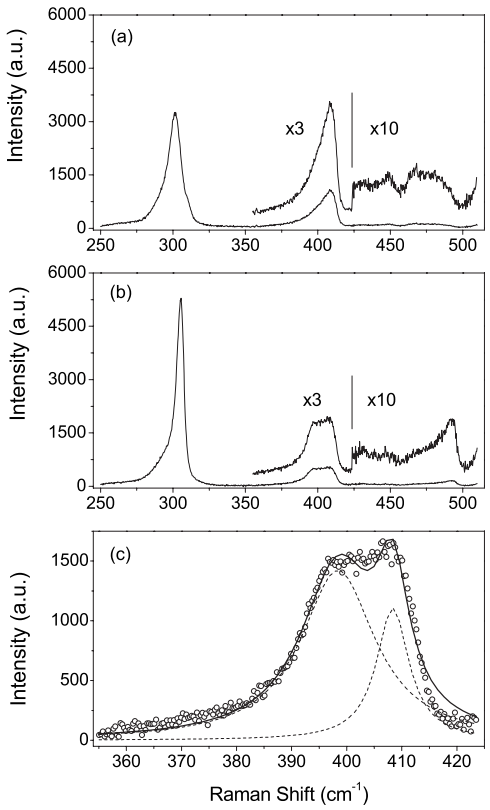

FIG. 3. Raman spectra of the samples annealed at 1100 °C for 1 h (a), 3 h (b), and decomposed peaks of the Si–Ge vibration mode of the sample annealed at 1100 °C for 3 h (c).

consist of three main peaks due to nearest-neighbor Ge–Ge (~300 cm^{-1}), Si–Ge (~400 cm^{-1}), and Si–Si (~500 cm^{-1}) stretching vibrations.[29] The latter is weak in Ge-rich alloys and is also masked by the intense peak coming from the Si substrate. Assuming random mixing in the alloy, from the relative integrated intensities of the Ge–Ge and Si–Ge peaks,[30] the Ge composition of $Si_{(1-x)}Ge_x$ structure can be found by using the following expression:

$$\frac{I_{\text{Ge–Ge}}}{I_{\text{Si–Ge}}} = \frac{n_{\text{Ge–Ge}} + 1}{n_{\text{Si–Ge}} + 1} \frac{\omega_{\text{Si–Ge}}}{\omega_{\text{Ge–Ge}}} \frac{x^2}{2x(1-x)}. \quad (3)$$

$I_{\text{Ge–Ge}}$ and $I_{\text{Si–Ge}}$ were obtained by integrating the areas under each peak and the $n_{\text{Ge–Ge}}$ and $n_{\text{Si–Ge}}$ are the Bose factors for the Ge–Ge and Si–Si phonon modes and ω's are the frequencies of these different modes. The third term represents the relative fraction of bonds in the alloy. For the sample annealed at 1100 °C for 1 h the Ge content of x was found to be 0.65. This composition homogeneity changes by increasing annealing time, which can be interpreted as a phase separation. From the XRD measurements, the value of 0.69 is obtained as given above. These two values obtained from Raman and XRD analysis are in agreement with each other. However, based on assumptions in both techniques, estimating the Ge composition has uncertainties. For instance as discussed in the previous section, XRD data predicts the presence of a strain in the nanocrystals opposed to the assumption made in the calculation of Ge composition by XRD.

As we know, there are three main factors that affect the Raman frequencies of the $Si_{(1-x)}Ge_x$ alloy, Ge content, stress, and phonon confinement effect. While relaxed $Si_{0.35}Ge_{0.65}$ alloy has Ge–Ge and Si–Ge vibration modes located at 293.4 and 406.3 cm^{-1}, respectively,[31] in our sample annealed at 1100 °C for 1 h these are located at 301.5 and 408.7 cm^{-1}, respectively [Fig. 3(a)]. This shift toward higher wave numbers can result from the compressive stress on the SiGe nanocrystals due to the stretching of Si–Ge bonds with respect to relaxed SiGe occurring near the interface of nanocrystals and SiO_2 matrix. As discussed early in XRD section, the stress resulted from volume expansion of SiGe during cooling down process can affect the Raman vibration modes as well. This effect will be more influenced in the sample for extended annealing. We note that, phonon confinement effect, which is evident only for the crystallite sizes <10 nm, in our sample with the mean crystallite size of 22 nm, it does not have significant effect on the shift in phonon modes.

Comparing Raman spectra of the samples annealed at 1100 °C for 1 and 3 h, we see that, while the intensity of the Ge–Ge vibration mode increases and shifts to higher wave number, the intensity of the Si–Ge vibration mode decreases. More interestingly, in the samples annealed for 3 and 5 h, the Raman peak has a flat top indicating the presence of inhomogeneous SiGe structure consist of different compositions. The observed Raman peak can be approximately deconvoluted into two Lorentzian type peaks as shown in Fig. 3(c). Regarding the shift in Si–Ge vibration mode toward lower wave numbers by increasing Ge content,[32] we attributed the low energy side of the doublet located at 398.4 cm^{-1} to the Ge–rich SiGe shell and the other at 408.4 cm^{-1} to the Si-rich SiGe core. Enlarged peaks in the range of 420–470 cm^{-1} appear in the Raman spectra of all c-$Si_{(1-x)}Ge_x$ samples whether they are MBE or liquid phase epitaxy grown, superlattices or single epitaxial layers, or bulk polycrystalline alloys. The weak peak located at ~430 cm^{-1} is generally assigned to another Si–Ge phonon peak and the others observed at ~450 and ~470 cm^{-1} to localized Si–Si vibration mode in the neighborhood of three and two Ge atoms, respectively.[29] In the spectra of the sample annealed for 3 h, these two latter peaks are weakened accompanied with the appearance of a relatively intense peak at 493 cm^{-1}, that is, Si–Si vibration mode with one neighboring Ge atom.[29] This phenomenon together with the decreased intensity of Si–Ge mode accompanied by increased intensity of Ge–Ge mode of the sample annealed for 3 h, and flat top feature of the Si–Ge signal all indicating strongly a phase separation in the SiGe nanocrystals when annealed for long enough time.

In this paper, our attention is focused on the evolution of SiGe nanocrystals during high temperature annealing. It is clear from our data that early in the annealing SiGe nanocrystals are formed and their composition appears to be uniform, which is in accordance with the observations of other groups.[7,8] However, partial or complete separation of Si and Ge from each other takes place in the system upon extended annealing at the high temperature. We attribute this phase separation to the formation of a core-shell structure with a Si-rich SiGe core surrounded by a Ge-rich SiGe shell. When discussing the core-shell character of the SiGe nanocrystals we should take into account contribution of different factors. First of all, because of its larger size, Ge atoms would induce local strains inside the structure. Thus it would be energetically more favorable for Ge atoms to stay on the surface of the islands. Another factor that might give rise to the core-shell structure is that most of the Ge atoms are members of five-number rings whereas all the Si atoms belong at least to one six-number ring. Participation of Ge atoms in the surface of the islands suggest that the difference in the cohesive energy can partly be explained by the lower dangling bond energy, and thus also lower surface energy of Ge. Surface segregation of the Ge atoms in SiGe clusters were studied by Tarus *et al.*[9] by using two different simulation methods: continuous-space Monte Carlo and analytical potential molecular dynamics. They found that the difference in atomic sizes, surface energy and elastic constants all contribute to the segregation effect, with the former two being more dominant. Furthermore, in a theoretical work, Asaduzzaman *et al.*[10] studied the electronic properties of (Si)Ge and (Ge)Si (core-)shell nanoparticles by using density-functional tight-binding method. They showed that the former is more stable than the other because of the lower surface energy of the Ge compared with that of Si. Additional strong support for core-shell model can be provided by looking at the surface mobility of Si and Ge. Recently, Huang *et al.*,[33] based on the first-principles calculations, studied the surface mobility difference between Si and Ge and its effect on the growth of SiGe alloy films and islands. They showed that Ge surface diffusion is generally faster than Si and that the surface mobility of different species exhibits a strong dependence on strain. Further, they showed that the surface diffusion disparity between Si and Ge is greatly enhanced on the island surface compared to that on a smooth layer surface.

IV. CONCLUSIONS

In summary, we have studied $SiO_2/SiO_2:Si:Ge/SiO_2$ sandwich films prepared by rf magnetron cosputtering method to understand the influence of the annealing time and temperature on the properties of nc-SiGe embedded in SiO_2 matrices. We have observed a uniform SiGe nanocrystal formation upon annealing at relatively low temperatures and short annealing time. However, by increasing annealing time from 1 to 3 h, in samples with higher Ge content the compositional uniformity is found to be disturbed. Segregation of Si and Ge atoms has been observed with XRD, Raman, and TEM measurements, consistently. We interpreted this as a phase separation in SiGe nanocrystals leading to the formation a Si-rich SiGe core covered by a relatively Ge-rich SiGe shell. This experimental observation is consistent with the result of reported theoretical and simulation methods.

ACKNOWLEDGMENTS

This work has been partially supported by the EU FP6 projects SEMINANO under the Contract No. NMP4 CT2004 505285 and METU-CENTER with Contract No. 17125. One of the authors (N.A.P.M.) would like to thank the Turkish Ministry of Education and TÜBİTAK (The Scientific & Technological Research Council of Turkey) for financial sup-

port. The authors wish to thank Yildiz I of the METU Central Laboratory for his help in XPS measurements.

[1]D. J. Lockwood, *Light Emission in Silicon: From Physics to Devices* (Academic, San Diego, 1998).
[2]A. Rodriguez, M. I. Ortiz, J. Sangrador, T. Rodriguez, M. Avella, A. C. Prieto, J.Jimenez, A. Kling, and C. Ballesteros, Phys. Status Solidi A **204**, 1639 (2005).
[3]D.-W. Kim, T. Kim, and S. K. Banerjee, IEEE Trans. Electron Devices **50**, 1823 (2003).
[4]I. B. Akca, A. Dana, A. Aydinli, and R. Turan, Appl. Phys. Lett. **92**, 052103 (2008).
[5]O. Nur, M. Karlsteen, M. Willander, R. Turan, B. Aslan, M. O. Tanner, and K. L. Wang, Appl. Phys. Lett. **73**, 3920 (1998).
[6]L. J. Lauhon, M. S. Gudiksen, D. Wang, and C. M. Lieber, Nature (London) **420**, 57 (2002).
[7]J. G. Zhu, C. W. White, J. D. Budai, S. P. Withrow, and Y. Chen, J. Appl. Phys. **78**, 4386 (1995).
[8]S. Takeoka, K. Toshikiyo, M. Fujii, S. Hayashi, and K. Yamamoto, Phys. Rev. B **61**, 15988 (2000).
[9]J. Tarus, M. Tantarimaki, and K. Nordlund, Nucl. Instrum. Methods Phys. Res. B **228**, 51 (2005).
[10]A. M. Asaduzzaman and M. Springborg, Phys. Rev. B **74**, 165406 (2006).
[11]Y. H. Kuo, Y. K. Lee, Y. Ge, S. Ren, J. E. Roth, T. I. Kamins, D. A. B. Miller, and J. S. Harris, Nature (London) **437**, 1334 (2005).
[12]A. Kolobov, H. Oyanagi, N. Usami, S. Tokumitsu, T. Hattori, S. Yamasaki, K. Tanaka, S. Ohtake, and Y. Shiraki, Appl. Phys. Lett. **80**, 488 (2002).
[13]Y. M. Yang, X. L. Wu, G. G. Su, G. S. Huang, J. C. Shen, and D. S. Hu, J. Appl. Phys. **96**, 5239 (2004).
[14]M. I. Alonso, M. D. Calle, J. O. Osso, M. Garriga, and A. R. Goni, J. Appl. Phys. **98**, 033530 (2005).
[15]A. Malachias, S. Kycia, G. Medeiros-Ribeiro, R. Magalhaes-Paniago, T. I. Kamins, and R. S. Williams, Phys. Rev. Lett. **91**, 176101 (2003).
[16]M. Y. Valakh, V. O. Yukhymchuk, V. M. Dzhagan, O. S. Lytvyn, A. G. Milekhin, O. P. Pchelyakov, F. Alsina, and J. Pascual, Nanotechnology **16**, 1464 (2005).
[17]I. N. Demchenko, K. Lawniczak-Jablonska, S. Kret, A. V. Novikov, J. Y. Laval, M. Zak, A. Szczepanska, A. N. Yabloskiy, and Z. F. Krasilnik, Nanotechnology **18**, 115711 (2007).
[18]E. S. Marstein, A. E. Gunnaes, A. Olsen, T. G. Finstad, R. Turan, and U. Serincan, J. Appl. Phys. **96**, 4308 (2004).
[19]J. D. Verhoeven, *Fundamentals of Physical Metallurgy* (Wiley, New York,1975), p. 400.
[20]Y. Maeda, Phys. Rev. B **51**, 1658 (1995).
[21]W. K. Choi, H. G. Chew, V. Ho, V. Ng, W. K. Chim, Y. W. Ho, and S. P. Ng, J. Cryst. Growth **288**, 79 (2006).
[22]K. H. Heinig, B. Schmidt, A. Markwitz, R. Grotzschel, M. Strobel, and S. Oswald, Nucl. Instrum. Methods Phys. Res. B **148**, 969 (1999).
[23]H. Fukuda, T. Kobayashi, T. Endoh, and Y. Ueda, Appl. Surf. Sci. **130–132**, 776 (1998).
[24]Y. Tu and J. Tersoff, Phys. Rev. Lett. **98**, 096103 (2007).
[25]C. Lang, S. Kodambaka, F. M. Ross, and D. J. H. Cockayne, Phys. Rev. Lett. **97**, 226104 (2006).
[26]J. P. Dismukes, L. Ekstrom, and R. J. Paff, J. Phys. Chem. **68**, 3021 (1964).
[27]F. Sanchez-Bajo and F. L. Cumbrera, J. Appl. Crystallogr. **30**, 427 (1997).
[28]E. Kasper and K. Lyutovich, *Properties of Silicon Germanium and SiGe: Carbon* (INSPEC, London, 2000) p. 48.
[29]M. I. Alonso and K. Winer, Phys. Rev. B **39**, 10056 (1989).
[30]M. A. Renucci, J. B. Renucci, and M. Cardona, *Proceeding of the Second International Conference on Light Scattering in Solids* (Flammarion, Paris, 1971), p. 326.
[31]H. K. Shin, D. J. Lockwood, and J. M. Baribeau, Solid State Commun. **114**, 505 (2000).
[32]S. Rath, M. L. Hsieh, P. Etchegoin, and R. A. Stradling, Semicond. Sci. Technol. **18**, 566 (2003).
[33]L. Huang, F. Liu, G. H. Lu, and X. G. Gong, Phys. Rev. Lett. **96**, 016103 (2006).